

Structural Properties of Prepared PANI/TiO₂ Nanocomposite by Chemical Polymerization

Noor K. Abid^{1a*}, Salma M. Hasan^{1b}

¹Department of Physics, College of Science, University of Baghdad, Baghdad, Iraq

^bE-mail: salma.muhammed@yahoo.com

^{a*}Corresponding author: noor.kadhumi.abid@gmail.com

Abstract

A progression of Polyaniline (PANI) and Titanium dioxide (TiO₂) nanoparticles (NPs) were prepared by an in-situ polymerization strategy within the sight of TiO₂ NPs. The subsequent nanocomposites were analyzed using Fourier-transform infrared spectra (FTIR), X-ray diffraction (XRD), Scanning Electron Microscopy (SEM), and Energy Dispersive X-Ray Analysis (EDX) taken for the prepared samples. PANI/TiO₂ nanocomposites were prepared by various compound materials (with H₂SO₄ 0.3 M and without it, to compare the outcome of it) by the compound oxidation technique using ammonium persulfate (APS) as oxidant within the sight of ultrafine grade powder of TiO₂ cooled in an ice bath. Nanocomposites were prepared by the addition of TiO₂ with two weight ratios (0.3 and 0.5 wt. %) during the polymerization of PANI. The outcomes showed good collaboration between PANI and TiO₂. FTIR spectral shows a shift to higher wave numbers in the peaks of PANI/TiO₂ nanocomposites, due to the Coulomb force that resulted from the interaction between the TiO₂ nanoparticles with PANI. SEM results show that the TiO₂ nanoparticles enwrap the polyaniline and agglomeration of uneven distribution of TiO₂ particles can be seen in the PANI matrix. The intensity of the peak in the EDX analyses was found to appear by adding the nanoparticles. XRD pattern of PANI polymerization and PANITNCs shows that the TiO₂ NPs and PANI affected the crystallization performance of nanocomposites, it was identified that the TiO₂ NPs form a relatively irregular distribution in the PANI chain.

Article Info.

Keywords:

TiO₂ nanocomposite, XRD, Polyaniline (PANI), In situ Polymerization, FTIR.

Article history:

Received: Jun. 27, 2022

Accepted: Aug. 17, 2022

Published: Sep. 01, 2022

1. Introduction

1.1. Polyaniline (PANI)

Polyaniline (PANI) is a renowned conductive polymer, and it got gigantic consideration from specialists in the areas of nanotechnology to improve sensors and optoelectronic devices. PANI is effectively doped with various acids because of its simple blend and amazing ecological stability [1]. Researchers have focused on creating conductive polymers that are accomplished in the fields of optics, devices, energy, etc. [2, 3]. PANI was known first as dark aniline and then came in various structures relying upon its oxidation levels. Moreover, PANI is known for its simplicity [4], natural steadiness, and capacity to be doped by protonic acids [5]. PANI is associating 1, 4-coupling of aniline monomer parts. PANI could exist in various oxidation states, and it may be described with the FTIR benzenoid to the quinonoid proportions [6]. Formed conductive polymers mainly include polyaniline (PANI), polythiophene (PTH), polypyrrole (PPY), and their items [7].

PANI has various potential applications including electromagnetic impedance protecting, photothermal treatment, battery-powered, photovoltaic cell, gas partition layer, substance sensor, anticorrosion covering, microwave ingestion, etc. [8, 9].

Moreover, conductive polymers are used, for example, leading fillers in protecting polymer substrates to gain directing polymer compounds [10-12]. These mixtures have possible applications in electromagnetic interference shields, electronic equipment, and display device electrodes [13]. PANI is a kind of material showing reflecting detection at room temperature and useful activity, this way is an appealing possibility for the improvement of various gas sensors. PANI properties, including its detecting qualities, were viewed as changed by dopants or by connection point collaboration in the composite [14].

1.2. Titanium Dioxide (TiO₂) Nanoparticles

The titanium dioxide (TiO₂) nanoparticles are a typical oxide metal, n-type of semiconductor that displays fascinating photocatalytic and some electronic properties that were able to open many promising applications in photograph voltaic, photocatalysis, photograph electrochromic, and sensors. TiO₂, particularly in the rutile structure, can oxidize natural materials straightforwardly because of its solid oxidative action. The presence of TiO₂ nanoparticles in the PANI lattice may cause a few changes and achieve some new fascinating properties [15]. Because of such presumptions, some research was done on the impact of the TiO₂ nanoparticles on gas detecting qualities of the PANI/TiO₂ blended by the in-situ method of synthetic polymerization [16].

2. Experimental

2.1. Materials and reagents

Aniline (ANI) C₆H₅NH₂ (AR, Beijing Chemical Reagent Co., China) was distilled and stored to use. Hydrophilic Rutile TiO₂ NPs Powder (Spec: 30-50 nm, 99.9%), ammonium persulfate (NH₄)₂S₂O₈ (APS, AR), and ethanol (AR) were used as oxidants as shown in Table 1.

Table 1: The name of the samples and percentage of the Nanoparticles.

<i>Sample name</i>	Nano present (TiO₂) %	Chemical materials
<i>H</i>	-	H ₂ SO ₄ /Aniline/Ammonium persulfate
<i>H1</i>	0.3	H ₂ SO ₄ /Aniline/Ammonium persulfate
<i>H2</i>	0.5	H ₂ SO ₄ /Aniline/Ammonium persulfate
<i>W</i>	-	Distilled water/Aniline/Ammonium persulfate
<i>W1</i>	0.3	Distilled water/Aniline/Ammonium persulfate
<i>W2</i>	0.5	Distilled water/Aniline/Ammonium persulfate

2.2. Preparation

Aniline 99.0% (ANI), TiO₂ NPs rutile, and ammonium persulphate (APS, Kanto Chemical Co. Inc.) were used as starting materials for synthesizing the PANI/ TiO₂ nanocomposites. Every one of the materials was used as received. The system was completed with various compound materials (with H₂SO₄ 0.3 M and without it) as follows: a solution of 10 ml of ethanol and different proportion of TiO₂ (as displayed

in Table 1) was on the stirrer for 30 min to make a solution of TiO₂. The TiO₂ solution was then treated with a solution of 0.5 ml aniline (0.1M) and 0.3 M H₂SO₄ (total solution 50ml). Then, a solution of 5 g ammonium persulphate with 50 ml distilled water was added dropwise to the ANI and TiO₂ solution blend. The two solutions were kept for 1 hr at 0 °C to polymerize. The solution was left to settle down until the following day. The precipitated PANI was gathered in filter papers. From that point onward, PANI powder was kept in a desiccator and left to dry in the air for about 3 days at room temperature to keep away from any impact of moisture absorption. The nanocomposite synthetic construction was investigated by FTIR, X-Ray diffraction analysis, Scanning Electron Microscopy (SEM), and Energy Dispersive X-Ray Analysis (EDX) taken for the prepared samples.

3. Result and discussion

3.1. FTIR studies

The most important peaks observed in the FTIR spectra of raw materials shown in Fig. 1 and the FTIR spectra of the PANI/TiO₂ nanocomposites (PANITNCs) were it contains (PANI 0.1 M water-based only) and (PANI 0.1 M with H₂SO₄ 0.3M) are shown in Fig. 2. Pure aniline characteristic peaks (in Fig.1) were observed at 965 cm⁻¹ C=C bending, 1141 cm⁻¹ C=N imines bending, the stretching mode 1295 cm⁻¹ C-N for benzenoid ring N=Q=N 1562 cm⁻¹ C=C for the quinoid ring, 1491 cm⁻¹ C=C benzenoid ring stretching N=B=N [17].

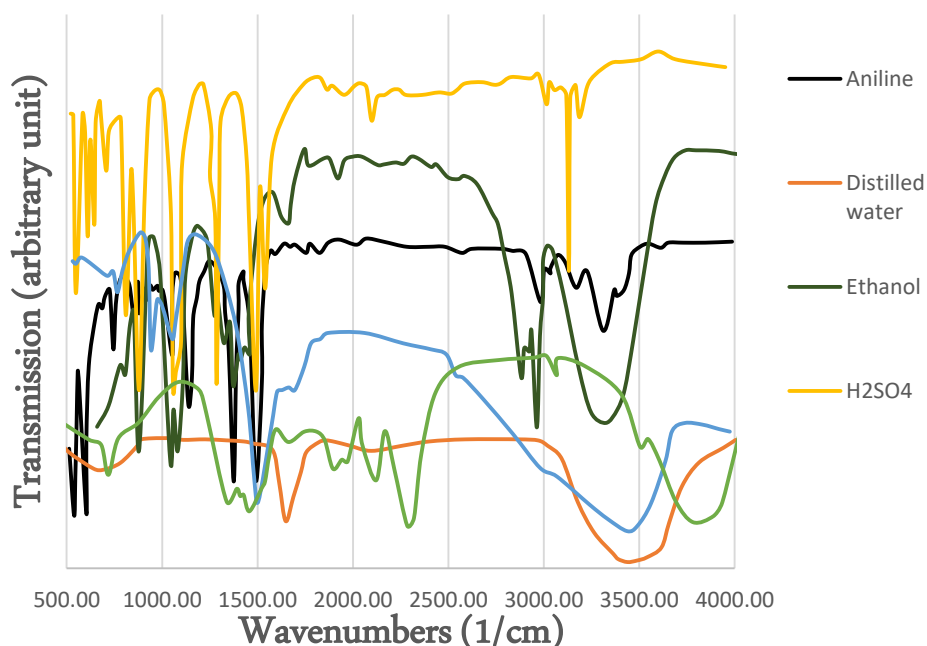


Figure 1: FTIR spectra of pure components.

The bands at 760 cm⁻¹, 680 cm⁻¹, 560 cm⁻¹, 500 cm⁻¹ and 468 cm⁻¹ are related to (Ti-O-Ti) vibrations [18]. From the FTIR spectrum of TiO₂ nanoparticles in Fig. 1, it can be seen that the bands for Ti-O and Ti-O-Ti bonds are available in the 800 - 400 cm⁻¹, the former being determined in a better wave number than the latter [19]. The 800 cm⁻¹ peak is assigned to a (Ti-O) vibration, in which the oxygen atom is in a non-binding situation.

The origins of the vibration bands are: the bands in the area 1114–1126 cm⁻¹ are because of in-plane bending vibrations of C–H mode of N=Q=N, Q=N H=B, and

B–N H–B, which is shaped for the duration of protonation. The stretching frequency at $3431\text{--}3456\text{ cm}^{-1}$ is of the NH of the aromatic amine. Areas at $2852\text{ to }2923\text{ cm}^{-1}$ are of CH vibration. The peaks in $1298\text{--}1301$, and $1242\text{--}1245\text{ cm}^{-1}$ belong to the C–N stretching of the benzenoid ring. Peaks at 1242 cm^{-1} indicate the protonated form of polyaniline. The PANI bands at 1558 , 1577 , and 1481 cm^{-1} belong to the C=N and the C=C modes of vibrations for quinonoid and benzenoid [20].

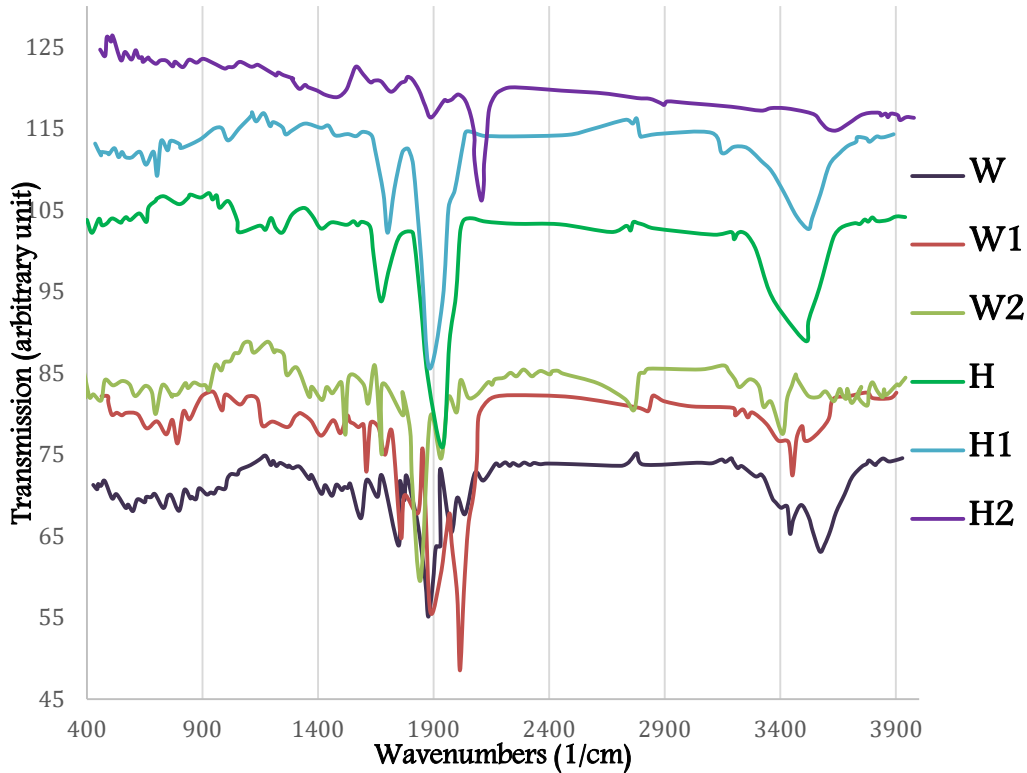


Figure 2: FTIR spectra of the pure PANI with H_2SO_4 (H), without it (W), PANITNCs W1, H1(0.3%), and W2, H2(0.5%).

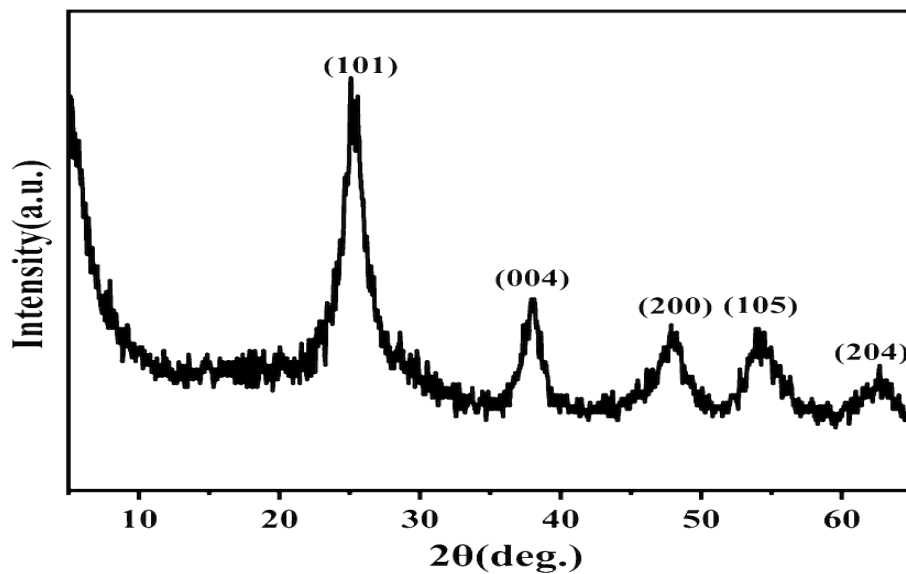
The results of FTIR demonstrated a shift of the peaks of PANI/TiO₂ nanocomposites to higher wave numbers due to the Coulomb force that resulted from the interaction between the TiO₂ nanoparticles and PANI, confirming that the structural and morphological changes in the nanocomposites have occurred. These assignments of vibrational modes of PANI and nanocomposites bands are listed in Table 2.

3.3. X-Ray diffraction analysis

Fig. 3 shows the X-ray diffraction pattern for pure TiO₂. The TiO₂ NPs peaks appeared at 2θ values of 25.2854° , 37.8654° , 47.8217° , 53.3905° , 62.4606° , and 68.8698° correlated to Miller indices of (101), (004), (200), (105), (213), and (116). The high intensity peaks are 25.2854° , 37.8654° , and 47.8217° with d spacing 3.5181 \AA , 2.3732 \AA , and 1.8998 \AA .

Table 2: Peaks position in the PANITNCs (H, H1, H2, W, W1, and W2) and Assignments of vibrational modes.

Description of vibrations & stretching modes		Wavenumbers [cm ⁻¹]					
		H	H1	H2	W	W1	W2
Ti-O & Ti-O-Ti		464	420	460	532	468	437
	CH ₂ & C-H	648	649	646	696	698	696
		846	923	858	860	864	862
C-O-C		1043	1045	1012	1080	1043	1045
	C-N	1269	1294	1301	1298	1298	1298
CH ₃ & C-H	C=C	1409	1423	1423	1413	1415	1413
		1579	1573	1575	1510	1510	1512
	C=O	1724	1778	1647	1635	1735	1639
O-H & N-H		3431	3425	3436	3434	3267	3267

**Figure 3: XRD pattern of TiO₂ nanoparticles.**

These peaks, in Fig.3, confirm the TiO₂ degree of crystalline, which is confirmed with JCPDS card numbers 21-1272 [21]. The XRD patterns are correlated with the same articles explaining and confirming the preparation of TiO₂ NPs. The peak value of 25.654°, which is one of the peaks for TiO₂ NPs, its correlated crystalline plane was (101). The crystalline size for the samples was observed from the Scherrer equation (Eq. (1) below) [22]:

$$D = \frac{0.9 \lambda}{\beta \cos \theta} \quad (1)$$

where: λ is the wavelength and D is the crystallite size, β -is the FWHM (full width out half maximum) of the XRD peak. The average crystalline size calculated for the prepared TiO₂ NPs was around 12 nm. The pure PANI peaks showed that a small

peak is around $2\theta = 18.495$, 20.148 , and 25.195 , with a d spacing of 4.7933\AA , 4.4037\AA , and 3.5318\AA indicating the conducting PANI; this also confirms the low crystalline structure. The crystalline size of the PANI is around 11 nm, which was calculated from the Scherrer equation [23].

For PANI/TiO₂ nanocomposites, the peak of the pure TiO₂ NPs phase indicates the amorphous nature of nanocomposites. PANI is polycrystalline in structure as shown in Fig.4, which may be allocated to the scattering of PANI chain at d spacing. Ammonium persulfate is mixed to the preparation technique; polymerization happens initially on the surface of TiO₂ NPs due to the restrictive impact of the surface. Thereafter, crystalline PANI combines the crystalline behaviors of TiO₂ NPs to obtain a polycrystalline structure. Therefore, the degree of crystalline of PANI decreases, and the X-ray diffraction peaks revealed combined and decreased with TiO₂ NPs peaks, and then, cannot be distinguished [24].

Comparing pure TiO₂ and pure PANI with nanocomposites, it is clear that the XRD of the PANI/TiO₂ nanocomposites is not identical to the crystalline structure of those of TiO₂ NPs. This explains that PANI polymerization of TiO₂ NPs has affected the crystallization performance of nanocomposites, it was identified that the TiO₂ NPs form a relatively irregular distribution in the PANI chain. Tables 3 & 4 listed the values of (2θ) of the strong peaks for the pure PANI and the nanocomposites.

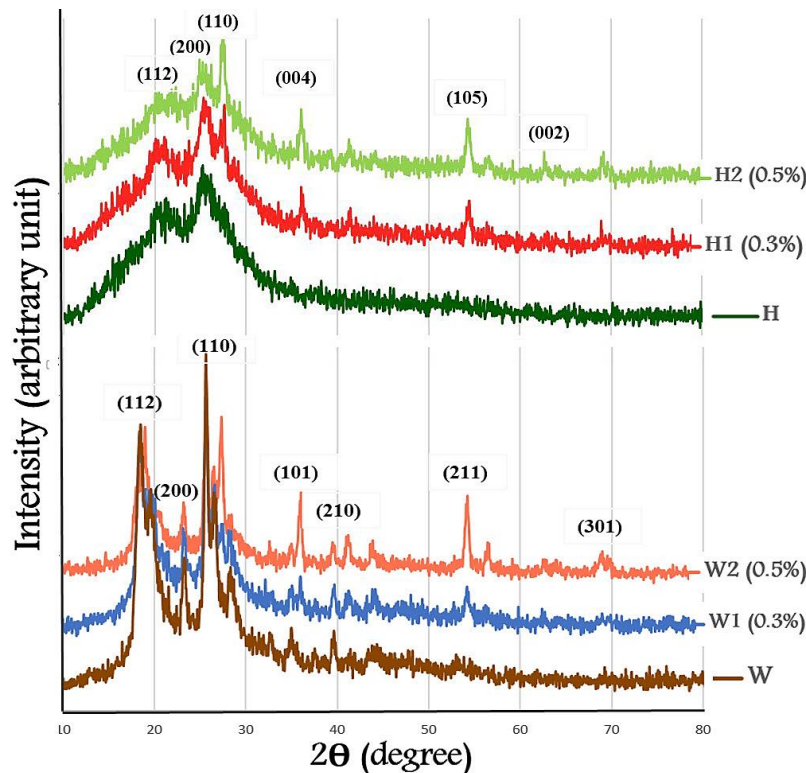


Figure 4: XRD patterns of the pure PANI with H₂SO₄ (H), without it (W), PANITNCs W1, H1 (0.3%), and W2, H2(0.5%).

Table 3: The values of (2θ) of the strong peaks of pure PANI with H_2SO_4 (H , PANITNCs H1(0.3%) and H2(0.5%).

Sample name	2Theta [Deg.]	d Exp.[Å]	FWHM [Deg.]	crystalline size [nm]
H	20.148	4.4037	0.72	11
	21.219	4.1837	0.246	33
	25.195	3.5318	0.83	9
	25.75	3.4569	1.113	7
H1	21.139	4.1994	0.117	72
	25.218	3.5286	0.819	9
	27.57	3.2327	0.231	35
	36.006	2.4923	0.26	32
	41.413	2.1785	0.122	71
	54.43	1.6843	0.362	24
	89.511	1.094	0.13	87
H2	24.856	3.5791	0.651	12
	25.537	3.4852	0.507	16
	27.444	3.2472	0.368	22
	36.005	2.4923	0.274	30
	41.257	2.1864	0.174	49
	44.16	2.0492	0.264	32
	54.248	1.6895	0.374	23
	56.568	1.6256	0.344	26
	62.665	1.4813	0.139	68

Table 4: The values of (2θ) of the strong peaks of the pure PANI with water based only (W), PANITNCs W1(0.3%) and W2(0.5%).

Sample name	2Theta [Deg.]	d Exp.[Å]	FWHM [Deg.]	crystalline size [nm]
W	18.495	4.7933	0.731	11
	23.251	3.8224	0.358	22
	25.654	3.4696	0.386	21
	26.548	3.3547	0.46	17
	28.348	3.1457	0.241	34
W1	19.843	4.4706	0.67	12
	25.654	3.4696	0.362	22
	32.938	2.7171	0.456	18
	35.985	2.4937	0.399	21
	39.692	2.2689	0.417	20
	48.058	1.8916	0.107	83

	49.317	1.8463	0.522	16
	54.193	1.6911	0.544	16
	68.956	1.3607	0.578	16
W2	18.993	4.6687	0.574	14
	20.032	4.4288	0.381	21
	27.347	3.2586	0.37	22
	36.038	2.4902	0.279	30
	41.19	2.1898	0.42	20
	43.89	2.0612	0.202	42
	54.247	1.6895	0.358	25
	56.585	1.6252	0.214	42
	63.944	1.4547	0.21	44
	68.801	1.3634	0.326	29

3.4. Scanning Electron Microscopy (SEM & EDX)

The morphologies of the pure PANI and 0.5 wt% TiO₂ (PANI/ TiO₂) nanocomposites were studied by SEM and EDX as shown in Fig.5. The SEM images show 2D nanosheet morphology. The nanocomposite sheets are rippled and crumpled, with dimensions ranging from 5 to 500 micrometers.

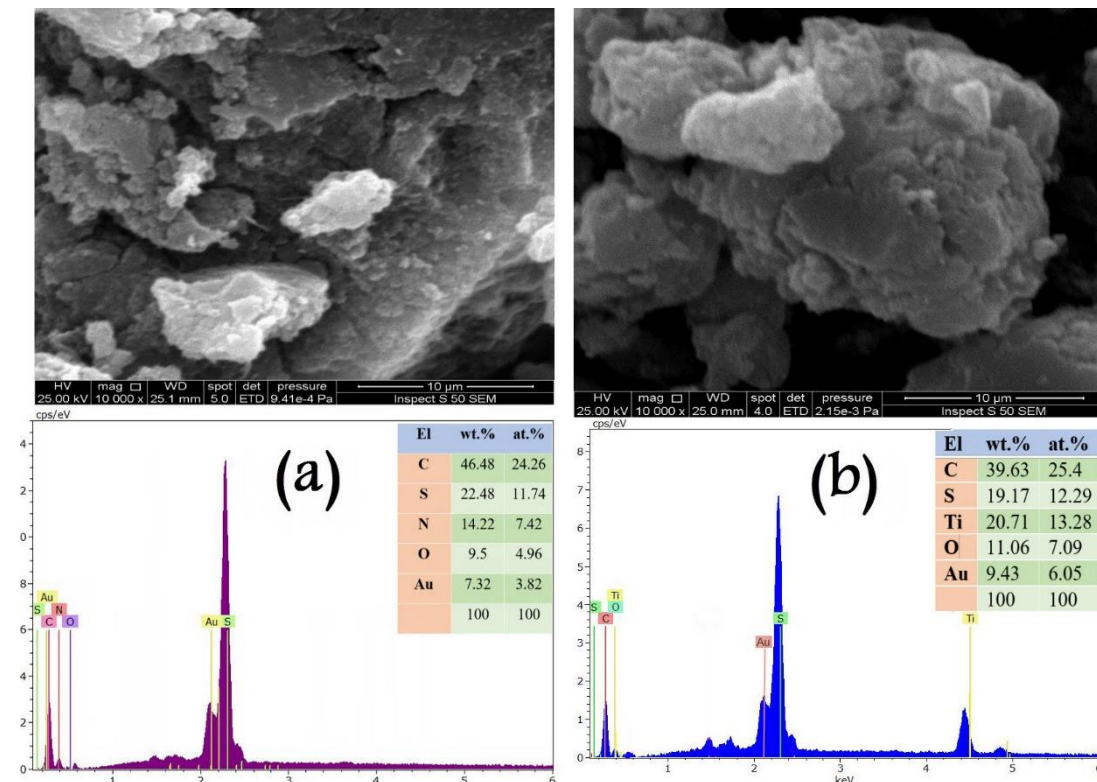


Figure 5: SEM images and DEX of (a) pure PANI (H) (b) PANI/TiO₂ (0.5%) (H2), prepared by chemical polymerization.

Fig. 5-a shows the SEM morphology of pure PANI film acquired in a solution containing 0.1 M aniline and 0.3 M H₂SO₄. From this figure, the spread PANI fibrils

are noticed, and the strands are ordinary and uniform. Additionally, these strands will generally agglomerate into interconnected networks, which show numerous multiple different pores [25].

Fig.5-b shows the SEM images of the (PANI/TiO₂) nanocomposites. The change in surface morphology is observed with the addition of TiO₂ (0.5%) in PANI. An agglomeration of uneven distribution of TiO₂ particles can be seen in the PANI matrix. The diffraction pattern from particles of nanocomposite suggests that the TiO₂ nanoparticles are deposited on the surface of PANI and show a typical rutile phase. The EDX analyses of the polymer and nanocomposite are also performed to confirm the incorporation of the nanoparticles in the PANI matrix. The intensity of the NPs in the nanocomposites peaks is found to appear by adding the nanoparticles.

4. Conclusions

PANI/TiO₂ nanocomposite was synthesized with the aid of using in-situ chemical polymerization by various substance materials (with H₂SO₄ 0.3 M and without it), and the resulting PANI and PANI/TiO₂ nanocomposite base on the water is less efficient when contrasted with doping by H₂SO₄. An acidic medium promotes the solubilization of the monomer, the aniline, in water and limits the secondary reactions. The nature of the acid influences the polymerization time, morphology, physicochemical properties, and molar mass. It was displayed in the attributes of PANI/TiO₂ by XRD and FTIR that the nanoparticles will generally fix along the PANI chain with expanding TiO₂ concentration. The nanocomposite results were obtained with FTIR studies, which confirmed the formation of PANI/TiO₂ nanocomposites. It showed a shift to higher wave numbers in the peaks of PANI/TiO₂ nanocomposites. XRD pattern showed that the TiO₂ NPs and PANI significantly affected the crystallization performance of nanocomposites. SEM images show that the TiO₂ NPs enwrap the polyaniline and agglomeration uneven distribution of TiO₂ NPs can be seen in the PANI matrix. It was identified that the TiO₂ NPs form a relatively irregular distribution in the PANI confirming that structural and morphological changes in the nanocomposites occurred.

Acknowledgments

The authors would like to thanks University of Baghdad/ College of Science/ Physics Department.

Conflict of interest

All authors declare that they have no conflicts of interest.

References

1. Beygisangchin M., Abdul Rashid S., Shafie S., Sadrolhosseini A.R., and Lim H.N., *Preparations, properties, and applications of polyaniline and polyaniline thin films—A review*. Polymers, 2021. **13**(12): pp.2003(1-46).
2. Najjar R., Katourani S.A., and Hosseini M.G., *Self-healing and corrosion protection performance of organic polysulfide@ urea-formaldehyde resin core-shell nanoparticles in epoxy/PANI/ZnO nanocomposite coatings on anodized aluminum alloy*. Progress in Organic Coatings, 2018. **124**: pp.110-121.
3. Liao G., Li Q., Zhao W., Pang Q., Gao H., and Xu Z., *In-situ construction of novel silver nanoparticle decorated polymeric spheres as highly active and*

- stable catalysts for reduction of methylene blue dye*. Applied Catalysis A: General, 2018. **549**: pp. 102-111.
4. Park C.S., Lee C., and Kwon O.S., *Conducting polymer based nanobiosensors*. Polymers, 2016. **8**(7): pp. 249(1-18).
 5. Bhadra J., Alkareem A., and Al-Thani N., *A Review of Advances in the Preparation and Application of Polyaniline Based Thermoset Blends and Composites*. Journal of Polymer Research, 2020. **27**(5): pp. 1-20.
 6. Gómez I.J., Vázquez Sulleiro M., Mantione D., and Alegret N., *Carbon nanomaterials embedded in conductive polymers: A state of the art*. Polymers, 2021. **13**(5): pp. 745(1-51).
 7. Brachetti-Sibaja S.B., Palma-Ramírez D., Torres-Huerta A.M., Domínguez-Crespo M.A., Dorantes-Rosales H.J., Rodríguez-Salazar A.E., and Ramírez-Meneses E., *CVD conditions for MWCNTS production and their effects on the optical and electrical properties of PPY/MWCNTS, PANI/MWCNTS nanocomposites by in situ electropolymerization*. Polymers, 2021. **13**(3): pp. 351(1-29).
 8. Liao G., *Green preparation of sulfonated polystyrene/polyaniline/silver composites with enhanced anticorrosive properties*. International Journal of Chemistry, 2018. **10**(1): pp. 81-86.
 9. Baker C.O., Huang X., Nelson W., and Kaner R.B., *Polyaniline nanofibers: broadening applications for conducting polymers*. Chemical Society Reviews, 2017. **46**(5): pp. 1510-1525.
 10. Sun E., Liao G., Zhang Q., Qu P., Wu G., Xu Y., Yong C., and Huang H., *Green preparation of straw fiber reinforced hydrolyzed soy protein isolate/urea/formaldehyde composites for biocomposite flower pots application*. Materials, 2018. **11**(9): pp. 1695(1-14).
 11. Li Q., Liao G., Tian J., and Xu Z., *Preparation of novel fluorinated copolyimide/amine-functionalized sepia eumelanin nanocomposites with enhanced mechanical, thermal, and UV-shielding properties*. Macromolecular Materials Engineering, 2018. **303**(2): pp. 1700407(1-14).
 12. Al-Oqla F.M., Sapuan S., Anwer T., Jawaid M., and Hoque M., *Natural fiber reinforced conductive polymer composites as functional materials: A review*. Synthetic Metals, 2015. **206**: pp. 42-54.
 13. Sobha A., Sreekala P., and Narayanankutty S.K., *Electrical, thermal, mechanical and electromagnetic interference shielding properties of PANI/FMWCNT/TPU composites*. Progress in Organic Coatings, 2017. **113**: pp. 168-174.
 14. Sinha S., Bhadra S., and Khastgir D., *Effect of dopant type on the properties of polyaniline*. Journal of Applied Polymer Science, 2009. **112**(5): pp. 3135-3140.
 15. Chen X. and Mao S.S., *Titanium dioxide nanomaterials: synthesis, properties, modifications, and applications*. Chemical Reviews, 2007. **107**(7): pp. 2891-2959.
 16. Kalaiarasi J., Balakrishnan D., Al-Keridis L.A., Al-mekhlafi F.A., Farrag M.A., Kanisha C.C., Murugan M., and Pragathiswaran C., *Sensing and antimicrobial activity of polyaniline doped with TiO₂ nanocomposite synthesis and characterization*. Journal of King Saud University-Science, 2022. **34**(3): pp. 101824(1-8).

17. Yasir M., *Optical properties and AC conductivity of PANI-ZnO nanocomposites*, M.Sc., Department of Physics, College of Science, Baghdad University, 2015.
18. Djaoued Y., Badilescu S., Ashrit P., and Robichaud J., *Vibrational properties of the sol-gel prepared nanocrystalline TiO₂ thin films*. The Internet Journal of Vibrational Spectroscopy, 2001. **5**(6): pp. 4.
19. Burgos M. and Langlet M.J.T.S.F., *The sol-gel transformation of TIPT coatings: a FTIR study*. Thin solid films, 1999. **349**(1-2): pp. 19-23.
20. Kang E., Neoh K., and Tan K., *Polyaniline: A polymer with many interesting intrinsic redox states*. Progress in Polymer Science, 1998. **23**(2): pp. 277-324.
21. Ramalingam S., *Synthesis of nanosized titanium dioxide (TiO₂) by sol-gel method*. International Journal of innovation technology exploring engineering, 2019. **9**(2S2): pp. 732-735.
22. Vella Durai S.C., Kumar E., Muthuraj D., and Bena Jothy V., *Investigations on structural, optical, and AC conductivity of polyaniline/manganese dioxide nanocomposites*. International Journal of Nano Dimension, 2019. **10**(4): pp. 410-416.
23. Mostafaei A. and Zolriasatein A., *Synthesis and characterization of conducting polyaniline nanocomposites containing ZnO nanorods*. Progress in Natural Science: Materials International, 2012. **22**(4): pp. 273-280.
24. Rajakani P. and Vedhi C., *Electrocatalytic properties of polyaniline-TiO₂ nanocomposites*. International Journal of Industrial Chemistry, 2015. **6**(4): pp. 247-259.
25. Antar A., Naimi Y., and Takky D., *Development of nickel-cobalt bimetallic/conducting polymer composite used as a catalyst in the oxygen evolution reaction (OER)*. IOP Conference Series: Earth and Environmental Science, 2018. **161**(1): pp. 012027(1-11).

الخصائص التركيبية لمتراكب نانوي محضر من PANI/TiO₂ بواسطة البلمرة الكيميائية

نور كاظم عبد¹، سلمى محمد حسن¹
¹قسم الفيزياء، كلية العلوم، جامعة بغداد، بغداد، العراق

الخلاصة

تم تحضير المتراكب النانوي المتكون من البولي انيلين (PANI) وثاني أكسيد التيتانيوم (TiO₂) من خلال استراتيجيات البلمرة في الموقع بإضافة الجسيمات النانوية TiO₂. تم تحليل المتراكبات النانوية (PANI / TiO₂) الناتجة باستخدام أطياف الأشعة تحت الحمراء (FTIR) وحيود الأشعة السينية (XRD) والفحص المجهر الإلكتروني (SEM) وتحليل الأشعة السينية المشتتة للطاقة (EDX) المأخوذة للعينات المعدة. تم تحضير نسب مختلفة من الـ PANI: TiO₂ بواسطة تقنية الأكسدة الكيميائية باستخدام بيرسلفات الأمونيوم (APS) كمؤكسد بوجود الجسيمات النانوية من TiO₂ المبرد في حمام جليدي. تم تحضير المتراكبات النانوية بإضافة نسبتيين من TiO₂ هما (3.0 و 5.0 %) غرام أثناء عملية بلمرة البولي انيلين. أظهرت النتائج توافقاً جيداً بين PANI و TiO₂ حيث يظهر طيف FTIR انحرافاً نحو الأعداد الموجية الأعلى في قمم المتراكبات النانوية PANI / TiO₂، بسبب قوة كولوم الناتجة عن التفاعل بين جسيمات TiO₂ النانوية مع البولي انيلين. تُظهر نتائج فحص الـ SEM أن جسيمات TiO₂ النانوية تغلف البولي انيلين والتوزيع غير المتكافئ لجزئيات TiO₂ التي يمكن رؤيتها ضمن جزئيات البولي انيلين. تم العثور على شدة الذروة للجسيمات النانوية المضافة من خلال تحليل الـ EDX. يوضح تشخيص XRD لبلمرة PANI و PANITNCs أن الجسيمات النانوية TiO₂ و PANI لهما تأثير على أداء التبلور للمتراكبات النانوية، وقد وجد أن جسيمات TiO₂ النانوية تشكل توزيعاً غير منتظم نسبياً على طول سلسلة البولي انيلين.